





Development of Hybrid Compensators for Enhancing Power Quality in Electrical Distribution Systems Using Innovative Optimization Techniques

Vijaykumar Kamble * , Ajit Bansode **[†] , Tushar Waghmare *** , Kalyan Bamane **** 

* Department of Electrical Engineering, AISSMS Institute of Information Technology, Pune, Maharashtra, India

** Department of Electrical Engineering, JSPM, Jaywantrao Sawant College Of Engineering, Pune, Maharashtra, India

*** Department of Electrical Engineering, Govt. College of Engineering and Research, Awasari, Pune, Maharashtra, India

**** Department of Computer Engineering, D. Y. Patil College of Engineering, Akurdi, Pune, Maharashtra, India

(vijaykumar.kamble@aissmsioit.org, dr.ajitbansode@gmail.com, wtushar123@gmail.com, kdbamane@dypcoeakurdi.ac.in)

[†]Corresponding Author; Ajit Bansode, Department of Electrical Engineering, JSPM, Jaywantrao Sawant College of Engineering, Pune, Maharashtra, India, dr.ajitbansode@gmail.com

Received: 14.02.2025 Accepted: 17.03.2025

Abstract- A power quality (PQ) issue arises when voltage, current, or service interruptions fall below standards, causing equipment disruptions for end users. To streamline decisions regarding voltage and current, it is advisable to utilize custom power tools that are based on hardware controllers for optimal performance. Distribution Static Compensation (DSTATCOM) and Dynamic Voltage Restore (DVR) are highly effective solutions for addressing power quality challenges. A DVR adds voltage to the system with structural voltage, while DSTATCOM injects current to resolve power quality concerns. Acting as a shunt compensator, DSTATCOM can address problems like harmonics, current imbalance, and inrush currents. The Unified Power Quality Conditioner (UPQC) integrates DVR and DSTATCOM without using a standard DC interface. The comprehensive analysis underscores the effectiveness of each device as a viable solution for customized power needs. In distribution networks, power quality (PQ) issues include voltage sag, swell, harmonics, and power imbalances. To enhance voltage quality, we explored two control strategies: DSTATCOM and DVR. Randomly placing DSTATCOM and DG within the network is suboptimal. A bus with a low MBO is considered weak. DSTATCOM and DG can be utilized to optimize voltage profiles, reduce imbalances, and minimize line losses. A PI controller identifies errors between variables and desired set points. A fuzzy logic controller evaluates data sources continuously, dealing with vague informational signals, which can be challenging for simple control signals involving a controlled PWM inverter. This research introduces Monarch Butterfly Optimization (MBO) and Grey Wolf Optimization (GWO) algorithms for controlling three-phase, two-stage DSTATCOM and DVR systems.

Keywords: Power quality, DSTATCOM, DVR, UPQC, grid connected system, fuzzy logic.

1. Introduction

Power flow quality is crucial due to issues involving abnormal voltage or current. Consumers on the demand side express dissatisfaction with power quality, while utility distribution systems experience frequent blackouts and service interruptions. These issues result in substantial

financial losses stemming from downtime, decreased production, and unproductive workforces. To address these issues, power systems are being modernized with advanced technology to improve power quality. Among the most effective solutions currently available are hardware-controller-based custom power devices, including the Dynamic Voltage Restorer (DVR) and the Distribution Static

Compensator (DSTATCOM). Both devices operate on the principle of the Voltage Source Inverter (VSI). The Dynamic Voltage Restorer (DVR) enhances the system voltage by introducing voltage in alignment with it, while the Distribution Static Synchronous Compensator (DSTATCOM) injects current into the system to mitigate power quality issues. The analysis presents detailed findings to evaluate the effectiveness of each device as a tailored power solution.

Here, we have considered methods for improving voltage quality through the use of two distinct controller strategies for DSTATCOM & DVR. The controllers that are utilized are the fuzzy logic controller (FLC) and the proportional integral controller (PIC). A PI Controller processes and raises a planned variable to meet the benchmark when it notices a difference between the intended set point and the variable. In fluffy set documentations as capacities, the information signals are spoken to and fuzzified. In order to contrast with a bearer motion using a control pulse width modulator (PWM) inverter, they described how rules give yield stimulating signals at that point and de-fuzzify them into simple control signals.

Modern power systems are extremely complicated and must meet the increasing needs for power at reasonable prices and quality levels. Generating units should be placed away from where the power is used due to economic and environmental reasons. The reorganization of electrical utilities has heightened operational uncertainties within the system. Due to legislative restrictions on the transmission network's growth, stability margins were reduced, raising the possibility of blackouts and cascading outages. The challenge of managing power flows and voltage levels in alternating current (AC) transmission networks has been effectively addressed through the implementation of advanced high-power electronic controllers. The AC transmission system's adaptable operation allows for alterations to be made without putting undue load on the system.

1.1. DVR & DSTATCOM

In this paper, we explore methods to enhance voltage quality by employing two distinct controller strategies: The Dynamic Voltage Restorer (DVR) and the Distribution Static Synchronous Compensator (DSTATCOM). Random placement of DSTATCOM and Distributed Generation (DG) within the network is not an efficient approach. Additionally, buses with low Maximum Bus Overvoltage (MBO) were identified as weak buses. The proposed model utilizes the IEEE 33-bus real unbalanced distribution network as a complete system, with load flow analysis conducted using MATLAB software. By strategically designing DSTATCOM and DG, the voltage profile can be optimized, leading to a reduction in voltage imbalance and line losses. The implemented controllers are presented and compared with a Proportional-Integral Controller (PIC) and an Artificial Intelligence Controller (AIC). A PI controller identifies errors by measuring the difference between a variable and its desired set point. On the other hand, a fuzzy logic controller processes a series of data inputs iteratively, handling vague

or imprecise information expressed in linguistic terms. These inputs are often ambiguous and require conversion into precise control signals, which are adjusted dynamically using a Pulse Width Modulation (PWM) inverter.

The paper introduces control algorithms based on Monarch Butterfly Optimization (MBO) and Grey Wolf Optimization (GWO), applied to a three-phase, two-stage Distributed Static Compensator (DSTATCOM) and Dynamic Voltage Restorer (DVR). Initially, the weighted values of the active and reactive power components of the load currents are utilized in the proposed control strategy to generate reference source currents. The effectiveness of this approach is validated through implementation in MATLAB/Simulink.

The distribution STATCOM operates similarly to a transmission STATCOM, utilizing a VSC that is appropriately rated for its application. The VSC employed in a Distributed Static Synchronous Compensator (DSTATCOM) is classified as a Type 1 converter. It effectively regulates a stable direct current (DC) voltage across the capacitor while managing the amplitude of the injected AC voltage through Pulse Width Modulation (PWM) techniques. Advanced power semiconductor devices, including IGBT and IGCT, have largely replaced Gate Turn-Off Thyristors (GTO). Due to their rapid switching capabilities, IGBTs and IGCTs facilitate the implementation of sophisticated control strategies for applications such as flicker mitigation, active filtering through harmonic current injection, and load balancing via the injection of negative sequence currents [26].

One way to conceptualize DSTATCOM is as a regulated variable current source. To enhance the dynamic rating within the capacitive domain, the integration of a fixed capacitor or filter alongside a DSTATCOM is recommended. By integrating a DC/DC power conditioner on the by incorporating an energy storage solution, such as Superconducting Magnetic Energy Storage (SMES), on the DC side, the system gains the capability to supply real power to the network during transient disturbances or significant voltage sags.

The DVR functions as a series-connected device, similar to a Static Synchronous Series Compensator (SSSC). The primary purpose of a DVR is to mitigate or completely eliminate voltage sags that may affect sensitive equipment. Each module of the already-installed modular DVR has a 2 MVA rating. They are designed to rectify up to 35% of three-phase voltage sags in less than 0.5 seconds. The DVR is engineered to accommodate voltage sags exceeding 50% when such sags result from single-line-to-ground (SLG) failures and affect only a single phase. Capacitors normally need to store between 0.2 and 0.4 MJ of energy for each megawatt of load handled. A DVR is integrated in series with the feeder through a transformer. The LV winding is integrated with the converter system. A Dynamic Voltage Restorer (DVR) optimizes its functionality by primarily remaining in stand-by mode, thereby bypassing the need for a converter. Its primary purpose is to uphold voltage regulation at the load bus. The DVR activates and injects the necessary series voltage only upon the detection of a voltage

sag. As with an SSSC, a DVR needs to be shielded from the fault currents.

1.2. Objectives

1. Development of TCSC and SVC's impact on enhancing voltage profiles and lowering power losses in transmission networks.
2. Calculating real power, reactive power, and power losses for 33 buses and 57 bus systems, as well as evaluating the best bus position.
3. Using MBO optimization techniques, the DSTATCOM with PV-based DG distribution system design minimizes real power loss, voltage sag, damping, settling time, RMS value of corrected voltages, and THD for 33-bus and 57-bus systems. Using GWO and MBO algorithms to reduce voltage sag and swell, settling time, RMS value of corrected voltages, and THD, DVR and DSTATCOM are engineered for identical distribution systems that aim to lower real power losses.

2. Installation of TCSC and SVC in Transmission Framework

The management and execution of power systems often involve complex challenges associated with the nonlinear and nonconvex optimal power flow problem. Reactive power compensation on weak nodes can be effectively controlled to enhance the system's steady state and dynamic performance, improve the voltage profile and lowers the losses. Higher rated power electronic equipment for high voltage systems can now be designed thanks to advancements in power electronics. In fact, the Flexible AC Transmission System was introduced as a result of this.

In addition to regulating the flow of reactive and active power within an electrical network, FACTS devices such as SVC, TCSC, and UPFC can also facilitate the redistribution of power flow, even under conditions of significant network loading [1]. This eventually helps to reduce congestion in the network as a whole to confirm the viability and effectiveness of the suggested strategy. The IEEE-30 bus system, recognized for its standardization, comprises a total of 41 branches. and a base MVA of 100, was taken into consideration [13]. This test setup consists of four transformers, six generators and nine shunt VAR compensators (capacitors). The total control variables in this method are 24; 6 generation bus voltages; 5 active power output PG generators; four transformer tap settings; and nine shunt capacitors, each with 5 MVAR. The system has a total active power demand of 283.4 megawatts (MW) and a total reactive power demand of 126.2 megavolt-amperes reactive (MVAR). Figure 1 illustrates the schematic diagram of the TCSC and SVC for the test system.

The analysis is tested by varying the system's load in increments of 10% from base values to 40%.

The load at each bus is adjusted in increments of 10%, ranging from base values to a maximum of 40%, to assess the effects of load fluctuations on system performance. The

performance of the load variation and other system characteristics is examined using the NR load flow approach. Table 1 displays the change in voltage magnitude, Table 2 and Table 3 illustrate the variations in active power flow as the load increases, as well as the apparent power flow for the IEEE 30 bus system. Figure 2 illustrates that when the load is increased from the base value, the magnitude of voltage at the load buses decreases. And also Figure 3 shows flow variations and margin differences of voltage magnitude at a 40% load rise.

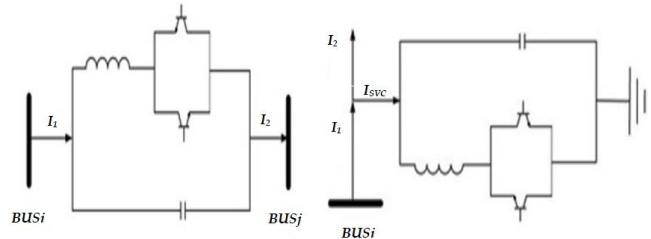


Fig.1. Schematic Diagram of TCSC and SVC for test system.

Table 1. Variation voltage magnitude with the increase in load for IEEE-30 bus system

Bus No.	Magnitude of Voltage (p.u)				
	Base Case	10% Demand	20% Demand	30% Demand	40% Demand
1	1.0706	1.0706	1.0706	1.0706	1.0706
2	1.0554	1.0554	1.0554	1.0554	1.0554
3	1.0393	1.0373	1.0363	1.0346	1.0322
4	1.0322	1.0302	1.0272	1.0252	1.0241
5	1.0201	1.0201	1.0201	1.0201	1.0201
6	1.0262	1.0252	1.0231	1.0211	1.0201
7	1.0161	1.0140	1.0120	1.0100	1.0090
8	1.0201	1.0201	1.0201	1.0201	1.0201
9	1.0635	1.0605	1.0575	1.0546	1.0524
10	1.0575	1.0524	1.0474	1.0423	1.0383
11	1.0928	1.0928	1.0928	1.0928	1.0928
12	1.0726	1.0696	1.0666	1.0635	1.0615
13	1.0817	1.0817	1.0817	1.0817	1.0817
14	1.0575	1.0524	1.0474	1.0423	1.0393
15	1.0524	1.0464	1.0413	1.0353	1.0322
16	1.0585	1.0544	1.0494	1.0443	1.0413
17	1.0524	1.0474	1.0413	1.0353	1.0322
18	1.0413	1.0353	1.0282	1.0211	1.0171
19	1.0383	1.0322	1.0252	1.0171	1.0130
20	1.0423	1.0363	1.0292	1.0221	1.0181
21	1.0454	1.0383	1.0322	1.0252	1.0211
22	1.0454	1.0393	1.0332	1.0262	1.0221
23	1.0403	1.0332	1.0272	1.0201	1.0151
24	1.0332	1.0262	LOOS	1.0100	1.0050
25	1.0272	1.0201	1.0130	1.0060	1.0009
26	1.0100	1.0009	0.9918	0.9817	0.9757
27	1.0332	1.0272	1.0211	1.0151	1.0110
28	1.0211	1.0191	1.0171	1.0151	1.0140
29	1.0130	1.0050	0.9969	0.9878	0.9827
30	1.0009	0.9918	0.9827	0.9726	0.9666

Table 2. Variation active power flow with increase in load for IEEE-30 bus system

Bus No.	Active / Real Power Flow in MW				
	Base Case	10% Demand	20% Demand	30% Demand	40% Demand
1	52.614	61.662	71.072	79.853	90.160
2	25.156	34.171	43.291	52.514	58.098
3	14.636	18.888	23.180	27.512	30.133
4	22.422	30.990	39.591	48.223	53.418
5	36.633	45.000	53.453	61.998	67.169
6	19.337	25.259	31.239	37.286	40.944
7	20.567	27.907	35.263	42.632	47.060
8	8.633	10.062	11.469	12.853	13.673
9	31.980	35.805	39.623	43.434	45.718
10	5.865	2.871	0.132	3.149	4.965
11	3.030	0.281	2.476	5.242	6.907
12	6.229	7.811	9.396	10.983	11.936
13	40.400	40.400	40.400	40.400	40.400
14	37.369	40.118	42.874	45.642	47.307
15	8.581	13.167	17.772	22.394	25.176
16	40.400	40.400	40.400	40.400	40.400
17	8.484	9.304	10.129	10.957	11.457
18	20.278	22.139	24.012	25.894	27.029
19	8.906	9.680	10.456	11.235	11.704
20	2.138	2.315	2.494	2.673	2.784
21	5.297	5.701	6.107	6.514	6.760
22	6.797	7.435	8.074	8.715	9.100
23	3.518	3.822	4.126	4.431	4.615
24	6.083	6.741	7.397	8.054	8.448
25	8.391	9.290	10.191	11.095	11.638
26	3.824	4.335	4.846	5.355	5.661
27	17.085	18.663	20.247	21.838	22.797
28	8.439	9.195	9.956	10.720	11.181
29	0.709	0.924	1.136	1.345	1.469
30	7.062	7.578	8.097	8.620	8.936
31	7.669	8.198	8.733	9.274	9.601
32	3.779	3.961	4.147	4.336	4.450
33	2.577	2.395	2.221	2.053	1.956
34	3.579	3.943	4.309	4.675	4.896
35	1.015	1.558	2.097	2.630	2.946
36	14.355	16.361	18.291	20.226	21.390
37	6.252	6.893	7.539	8.188	8.580
38	7.162	7.900	8.643	9.390	9.840
39	3.740	4.120	4.500	4.881	5.111
40	4.190	4.175	4.163	4.156	4.154
41	10.281	12.227	14.176	16.130	17.302

Table 3. Variation of apparent power flow with increase in load for IEEE-30 bus system

Bus No.	Apparent power flow (MVA)					Line Limit
	Base Case	10% Demand	20% Demand	30% Demand	40% Demand	
1	54.323	50.261	53.219	55.761	59.654	130
2	27.953	58.306	26.646	27.498	29.229	80
3	17.466	30.863	15.752	15.760	16.564	65
4	26.302	53.366	24.902	25.476	26.827	85
5	37.773	66.977	37.491	37.947	38.586	130
6	22.375	41.211	20.706	21.261	22.953	65
7	21.811	47.044	22.096	24.568	28.646	90
8	11.116	19.503	9.619	8.305	7.754	70
9	31.510	45.497	31.994	31.883	32.276	130
10	11.127	4.953	24.568	31.296	28.097	32
11	6.152	8.158	8.367	9.576	9.625	65
12	7.069	12.262	5.816	5.634	5.737	32
13	43.194	44.265	41.726	40.975	40.421	65
14	39.635	49.114	36.692	35.872	35.918	65
15	18.477	30.044	16.164	15.049	14.868	65
16	41.193	42.574	40.303	40.225	40.649	65
17	9.256	11.901	8.428	8.050	7.851	32
18	23.025	28.715	20.269	19.389	19.350	32
19	10.041	12.652	9.034	8.615	8.461	32
20	2.698	2.912	1.926	1.839	2.118	16
21	5.957	7.076	5.124	4.952	5.154	16
22	7.061	9.398	6.874	6.751	6.632	16
23	3.655	4.722	3.480	3.371	3.279	16
24	6.569	9.136	6.766	6.911	7.082	32
25	9.027	12.575	9.225	9.370	9.539	32
26	5.212	8.139	6.670	7.672	8.670	32
27	22.388	26.340	17.676	15.719	15.173	32
28	11.287	12.668	8.304	7.344	7.495	32
29	1.324	2.818	4.687	8.753	12.149	32
30	9.823	9.769	6.457	6.915	8.999	16
31	12.314	10.148	6.655	9.959	14.978	16
32	6.094	4.734	3.520	5.877	8.958	16
33	10.100	1.948	5.955	16.484	25.845	16
34	4.292	5.871	4.277	4.270	4.264	16
35	5.925	4.393	8.858	20.249	30.658	16
36	26.720	23.620	17.846	34.190	50.395	65
37	13.034	8.877	8.918	21.636	34.335	16
38	17.164	10.096	12.219	31.301	49.726	16
39	10.222	5.161	8.348	22.009	37.468	16
40	4.106	4.175	9.408	14.796	18.026	32
41	19.308	18.034	12.738	24.297	36.949	32

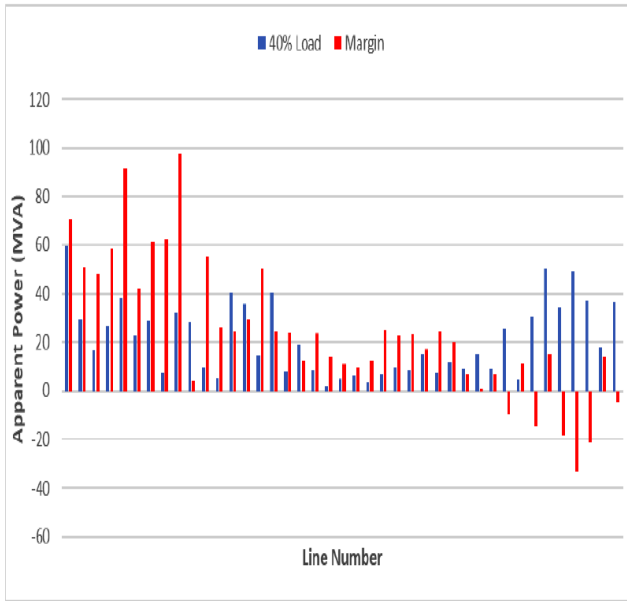


Fig. 2. Voltage variation for IEEE-30 bus systems as load increases.

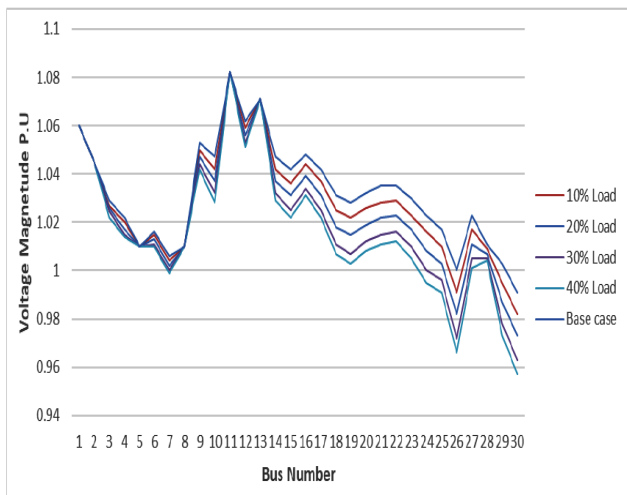


Fig. 3. Flow variations and margin differences at a 40% load rise.

3. Methodology

Distribution systems have comparatively higher power losses than power transmission networks. Therefore, minimizing power loss was one of the distribution network operator's initial objectives. One of the main objectives has been to control node nominal voltages. Furthermore, the aforementioned objectives can be most effectively accomplished when power networks have a dependable and effective energy source or component. Finding the optimal DGs based on RES control and demand variations for distribution networks has proven challenging. The upstream flow of power entering the system could be reversed by high renewable energy output during light load hours. As a result, the major grid could be considered a target when RES is being implemented. The typical construction of reverse electricity flow has been established, aiming to minimize

power losses, optimize voltage profiles, and facilitate backward power flow into the grid. Additionally, the paper seeks to achieve an optimal design for renewable energy sources, specifically photovoltaic systems and distributed generation.

To minimize the total real power loss in the distribution system, an objective function is formulated and defined as follows:

(i) Minimizing Real Power Loss

$$f_1 = \min \left(\sum_{i=1}^n S_i^{Total Losses} \right) \quad \text{--- (1)}$$

Subjected to

$$\begin{aligned} V_{min} &\leq V_i \leq V_{max} \\ |I_{i,i+1}| &\leq |I_{i,i+1,max}| \end{aligned}$$

$$\sum_{i=1}^n P_{Di} \leq \sum_{i=1}^n (P_i + P_{Loss(i,i+1)}) \quad \text{--- (2)}$$

Furthermore, given that active and reactive power constitute the total complex power, the losses associated with both reactive and active components can be articulated as shown below.

$$P_{k,Loss} = R_{m,k} \left(\frac{P_k^2 + jQ_k^2}{|V_m|^2} \right) \quad \text{--- (3)}$$

$$Q_{k,Loss} = X_{m,k} \left(\frac{P_k^2 + jQ_k^2}{|V_m|^2} \right) \quad \text{--- (4)}$$

Reactive power loss and active power loss for bus k are shown above, respectively.

It is possible to describe the target function to enhance the voltage profile as

$$f_2 = \sum_{i=1}^n (V_i - V_{ref})^2 \quad \text{--- (5)}$$

The constraints for the objective functions are as follows:

We must make sure that the bus voltages for the DG, DSTATCOM, and DVR are between 0.95pu and 1.05pu.

The branch currents should be less than the maximum branch current rating.

The location of DG, DSTATCOM and DVR must be at optimal location.

DG, DSTATCOM, and DVR should contribute less actual and reactive power to the distribution system than the system's peak demand.

The present spike in interest in DG could be due to the world's rising demand for electricity. In the past, DG has employed renewable energy sources like solar, wind, and photovoltaics as alternative energy sources [17]. Since DG has so many benefits, it is unable to release any harmful gases or pollutants. As electricity demand increases, distributed generation (DG) is essential for ensuring reliable

power backup solutions. The strategic injection of DG in the distributed network system reduces losses in line and mitigates voltage imbalances, thereby enhancing the overall voltage profile. This approach also diminishes the need for additional network capacitors and voltage regulators. To fully leverage the advantages of DG, meticulous planning is essential for its effective implementation within real-imbalance network distribution systems.

The term "DSTATCOM" refers to a static compensator utilized within a distribution network. It functions as a fixed synchronous compensator, akin to a shunt device, which helps regulate system voltage and substantially reduces the need for reactive power support [6]. The DSTATCOM is composed of a controller, a coupling reactor set, and a VSC, as illustrated in Figure 4. The system serves a critical function in managing voltage at the bus by either generating or absorbing reactive power within the network.

The variations in voltage across the reactance of the power supply and DSTATCOM will lead to both reactive and active power adjustments. The problem of voltage quality arises when the points of connection are common. D-STATCOM's performance at higher values offers the lowest ripple voltage and power compensation if the influence of the dc storage is enhanced. The electricity network has been linked to DSTATCOM.

The best place to put the DG will be on the bus that achieves the maximum value of the given objective function.

$$\max(f_1) = \omega_1 \times P_i + \omega_2 \times Q_i - \omega_3 \left\{ \sum_{m=1}^n (V_m - V_{min})^2 + (V_m - V_{max})^2 \right\} \dots (6)$$

The optimal location for the installation of distributed generation (DG) is determined by identifying the bus that maximizes the value of the objective function f1.

$$\min(f_2) = \left(\frac{P'_{Loss}}{P_{Loss}} \right) \times 0.01 + \left\{ \sum_{m=1}^n (V_m - V_{min})^2 + (V_m - V_{max})^2 \right\} \dots (7)$$

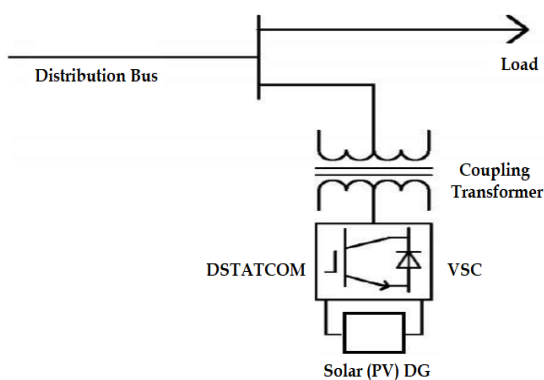


Fig. 4. DSTATCOM integrated with the IEEE 33-bus distribution network.

4. Results

The IEEE 33 radial distribution bus systems' base case findings are shown. The IEEE 33 bus test system comprises of 33 buses and 32 unique lines. The reactive power demand is measured at 2.3 MVAR, while the total real power demand stands at 3.715 MW. The base case study begins with the source (Bus1) serving as the reference bus and all buses' voltages at 1pu. Figure 5 displays the voltage curve, with the 18th bus having the lowest value.

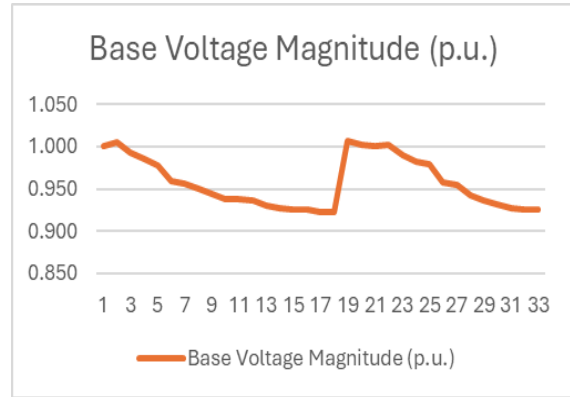


Fig. 5. Voltage profile of IEEE 33 Bus test system.

The total reactive power loss is measured at 143.12 kVAR, while the total real power loss amounts to 210.97 kW. Notably, the most significant losses are observed on line number two. Optimizing Distributed Generation through MBO Algorithm with Integrated DSTATCOM Allocation. The minimum voltage bus (18th) saw a voltage of 0.922 p.u., according to the load flow. The voltages of buses 6 to 18 and 26 to 33 have been low. The Monarch Butterfly Optimization (MBO) algorithm is employed to tackle the optimization challenges associated with the installation of DG alongside DSTATCOM, with the objective of minimizing power losses [11]. The MBO states that the ideal place to install the DSTATCOM for the 33 bus test system is on bus number 18. The ideal places will vary depending on the circumstances. Figure 6 displays the convergence characteristics of the simulation, which was also completed by installing DG with DSTATCOM.

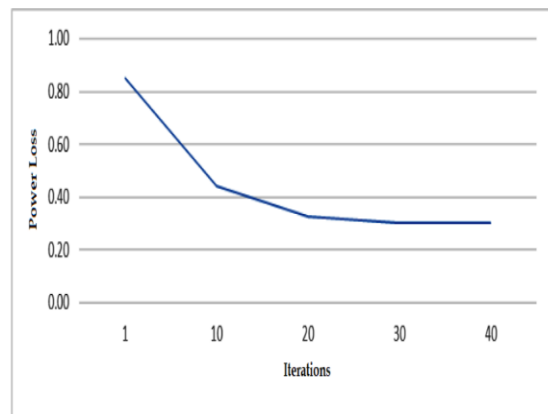


Fig. 6. Convergence characteristics for IEEE 33 bus test system.

Table 4. The results of the analysis of load flow for the IEEE 33 bus system

Bus No	Magnitude of Base Voltage (p.u.)	Angle in degrees
1	1.010	0.000
2	1.006	-0.006
3	0.993	-0.044
4	0.985	-0.084
5	0.978	-0.126
6	0.959	-0.064
7	0.956	-0.379
8	0.951	-0.739
9	0.945	-0.973
10	0.939	-1.188
11	0.938	-1.161
12	0.936	-1.112
13	0.930	-1.554
14	0.928	-2.024
15	0.926	-2.445
16	0.925	-2.738
17	0.923	-4.024
18	0.922	-0.075
19	1.007	-0.001
20	1.003	-0.011
21	1.001	-0.015
22	1.002	-0.024
23	0.989	0.000
24	0.982	-0.004
25	0.979	-0.008
26	0.957	0.002
27	0.955	0.003
28	0.943	0.005
29	0.936	0.006
30	0.931	0.008
31	0.927	0.001
32	0.926	-0.002
33	0.926	-0.005

Table 5. Line losses in IEEE 33 bus test system

Line No.	Real Power Loss (kW)	Reactive Power Loss (kVAr)
1	12.362	6.301
2	52.336	26.657
3	20.153	10.264
4	18.944	9.648
5	38.758	33.458
6	1.956	6.465
7	11.932	8.612
8	4.287	3.080
9	3.652	2.589
10	0.568	0.188
11	0.904	0.299
12	2.735	2.152
13	0.748	0.985
14	0.366	0.326
15	0.288	0.211
16	0.258	0.345
17	0.054	0.043
18	0.162	0.155
19	0.836	0.754
20	0.102	0.119
21	0.044	0.058
22	3.199	2.186
23	5.170	4.082
24	1.294	1.012
25	2.615	1.332
26	3.347	1.705
27	11.362	10.018
28	7.849	6.861
29	3.917	1.995
30	1.602	1.584
31	0.214	0.250
32	0.013	0.106

Table 6. Voltage magnitudes of IEEE 33 bus test system

Bus No	Base Case	DG	DSTAT COM	DG with DSTAT COM
1.	1.000	1.000	1.000	1.000
2.	0.999	0.998	0.998	0.997
3.	0.988	0.998	0.992	0.997
4.	0.980	0.999	0.987	0.998
5.	0.973	0.997	0.982	0.998
6.	0.954	0.991	0.971	0.997
7.	0.951	0.989	0.968	0.996
8.	0.946	0.987	0.964	0.994
9.	0.940	0.985	0.959	0.994
10.	0.934	0.983	0.955	1.000
11.	0.933	0.983	0.955	1.000
12.	0.931	0.983	0.953	0.994
13.	0.926	0.983	0.950	0.990
14.	0.923	0.983	0.948	0.990
15.	0.922	0.984	0.947	0.989
16.	0.920	0.983	0.946	0.988
17.	0.918	0.981	0.945	0.988
18.	0.918	0.980	0.945	0.989
19.	0.997	0.999	0.997	0.988
20.	0.997	1.000	0.999	0.985
21.	0.997	0.999	0.997	0.985
22.	0.997	0.999	0.997	0.984
23.	0.984	0.996	0.988	0.986
24.	0.977	0.990	0.981	0.991
25.	0.970	0.987	0.978	0.988
26.	0.953	0.989	0.968	0.988
27.	0.950	0.987	0.966	0.999
28.	0.939	0.976	0.955	0.989
29.	0.930	0.968	0.947	0.981
30.	0.927	0.960	0.943	0.977
31.	0.923	0.960	0.939	0.973
32.	0.922	0.959	0.938	0.972
33.	0.921	0.958	0.937	0.972

The obtained results for the IEEE 33 bus system are given in Table 4, Table 5, and Table 6, consequently. To enhance the system's functioning, DG is connected to the bus via DSTATCOM, which also raises the system's voltage profile. The ideal values for DG and DSTATCOM at bus 18 are 359.4kW and 692.1kVAr, respectively, and the simulation is run both independently and jointly.

The DSTATCOM is located at bus number 18, and the dynamic and reactive power generation in p.u. alongside the THD have been recorded using MATLAB flow features. The voltages are higher than base case values when DSTATCOM is attached at the ideal place. However, because they are at the tail end of the system, the voltages of a small number of buses (12 to 18 buses and 29 to 33 buses) have improved, although they are still below 0.95 p.u. Voltage profiles in a 33 bus test system for different cases are given in Figure 7.

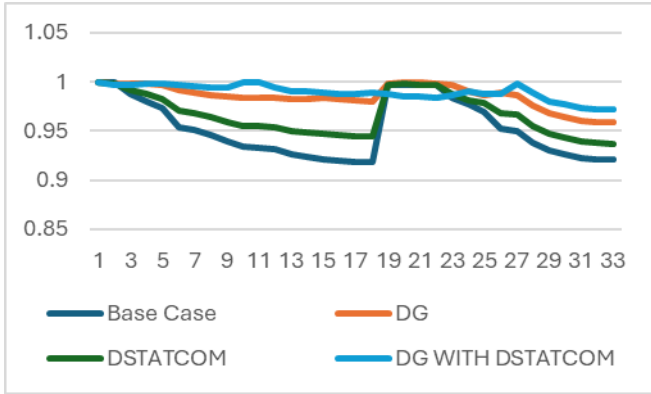


Fig. 7. Enhancing voltage profile in a 33-bus test system using distributed generation for compensation.

Line losses are observed to be 27.43kVAr and 30.13 kW. High losses are seen in the first line, but losses in line 2 are decreased to 3kW. A limited number of bus voltages, specifically those ranging from 12 to 18 and 29 to 33, fall below 0.95 per unit when utilizing DSTATCOM. Consequently, both systems are implemented concurrently, resulting in the anticipated enhancement in performance. Table lists the performance indexes that were taken into consideration. Performance metrics at optimal locations are given in Table 7. Voltage profiles at pcc for different cases of 33bus system are given in Figure 8, Figure 9, Figure 10 and Figure 11, consequently.

Table 7. Performance metrics associated with the strategic placement of devices at optimal locations.

	Base Case	DG	DSTATCOM	DG WITH DSTATCOM
Least voltage & bus	0.9132 pu at 18 th Bus	0.9545 pu at 33 rd bus	0.933 pu at 33 rd Bus	0.9675 pu at 33 rd Bus
Total Real Power losses	210.97kW	113.15kW	151.47kW	30.13kW
Total Reactive Power losses	143.12kVAr	102.33kVAr	89.8kVAr	27.43kVAr

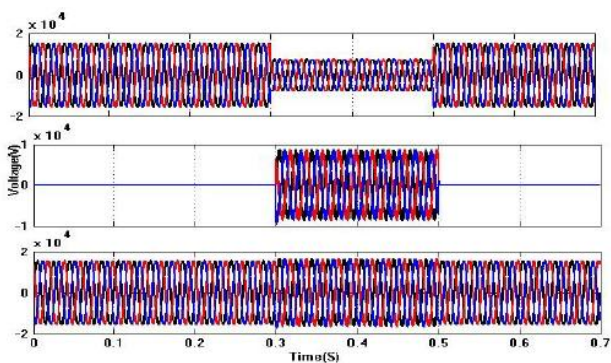


Fig. 8. Voltage profile (Vabc) at pcc: Sag voltage, DG based DSTATCOM injected voltage, compensated voltage at load 33 bus.

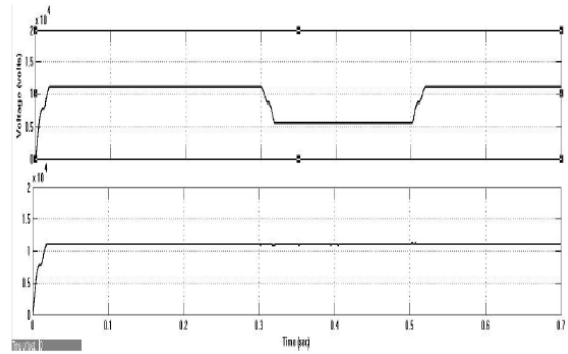


Fig. 9. Voltage profile (Vrms) at pcc: Before & After compensation (Sag) for 33 bus.

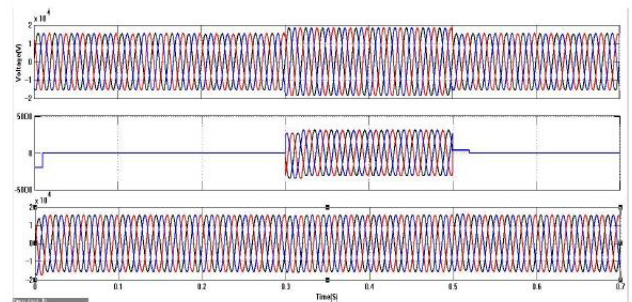


Fig. 10. Voltage profile (Vabc) at pcc: Swell voltage, DG based DSTATCOM injected voltage, compensated voltage at load for 33 bus.

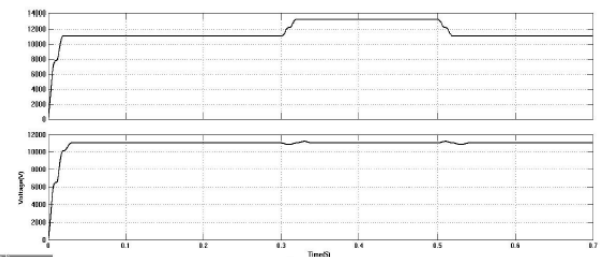


Fig. 11. Voltage profile (Vrms) at pcc: Before & after compensation (swell) for 33 bus.

5. Conclusion

This paper successfully implemented and evaluated the effectiveness of hybrid compensators, specifically DSTATCOM and DVR, in enhancing power quality within electrical distribution systems. The study leveraged advanced optimization techniques, including Monarch Butterfly Optimization (MBO) and Grey Wolf Optimization (GWO), to optimize compensator placement and minimize power losses.

Voltage Profile Improvement: The implementation of DG with DSTATCOM significantly improved the voltage profile across the IEEE 33-bus system. The lowest recorded voltage at bus 18 increased from 0.9132 p.u. (base case) to 0.9675 p.u. when both DG and DSTATCOM were optimally placed.

Reduction in Power Losses: Total real power losses were reduced from 210.97 kW (base case) to 30.13 kW when DG and DSTATCOM were integrated. Total reactive power

losses decreased from 143.12 kVAr to 27.43 kVAr, demonstrating the effectiveness of the optimization-based compensator placement strategy.

Voltage Sag and Swell Mitigation: The integration of DSTATCOM at the optimal location enhanced system stability by improving voltage correction during fluctuations, ensuring RMS voltage regulation within 0.95 to 1.05 p.u.

Line Loss Reduction: High-loss segments, such as line 2, showed a dramatic reduction in losses from 52.336 kW to 3 kW, demonstrating the improved efficiency of power distribution.

These findings validate the effectiveness of the proposed hybrid compensator framework, optimized through MBO and GWO algorithms. The study provides a scalable approach for improving power quality in distribution networks, reducing energy losses, and enhancing voltage stability, paving the way for future research in adaptive control strategies and real-time compensator deployment.

References

- [1] K. R. Padiyar, "Facts Controllers in Power Transmission and Distribution", New Age International Publishers, 2007.
- [2] J. Vuletić, and M. Todorovski, "Optimal capacitor placement in radial distribution systems using clustering based optimization", International Journal of Electrical Power & Energy Systems., vol.62, pp.229-236, 2014.
- [3] S. Devi, and M. Geethanjali, "Optimal location and sizing of Distribution Static Synchronous Series Compensator using Particle Swarm Optimization", International Journal of Electrical Power & Energy Systems., vol.62, pp.646-653, 2014.
- [4] S. Ganguly, "Impact of Unified Power-Quality Conditioner Allocation online Loading, Losses, and Voltage Stability of Radial Distribution Systems", IEEE Transactions on Power Delivery., vol.29, no.4, pp.1859-1867, 2014.
- [5] Ihsan Jabbar Hasan, Iman Subhi Mahmood, Qais Mohammed Aish, Aqeel A. Al-Hilali, Mohannad Jabbar Mnati, "Voltage Sag Mitigation Methods in Low Voltage Networks with Photovoltaic Units: Modelling and Analysis", International Journal of Renewable Energy Research, Vol.14, No.4, December, 2024.
- [6] S. A. Taher, and S. A. Afsari, "Optimal location and sizing of DSTATCOM in distribution systems by immune algorithm," International Journal of Electrical Power & Energy Systems., vol.60, pp.34-44, 2014.
- [7] K. R. Devabalaji, and K. Ravi, "Optimal size and siting of multiple DG and DSTATCOM in radial distribution system using Bacterial Foraging Optimization Algorithm", Ain Shams Engineering Journal., 2015.
- [8] S. A. Taher, and S. A. Afsari, "Optimal location and sizing of DSTATCOM in distribution systems by immune algorithm," International Journal of Electrical Power & Energy Systems., vol.60, pp.34-44, 2014
- [9] J. Sanam, S. Ganguly, and A. K. Panda, "Placement of DSTATCOM in radial distribution systems for the compensation of reactive power," In Smart Grid Technologies-Asia (ISGT ASIA), 2015 IEEE Innovative., pp.1-6, 2015.
- [10] T. Yuvaraj, K. Ravi and K. R. Devabalaji. "DSTATCOM allocation in distribution networks considering load variations using bat algorithm," Ain Shams Engineering Journal., 2015.
- [11] S. Muthubalaji, Vijaykumar Kamble, Vaishali Kuralkar, Tushar Waghmare, T. Jayakumar, "An innovative muted ant colony optimization (MAPO) controlling for grid PV system" International Journal of Information Technology, 2024.
- [12] M. Chalbi, R. Kallel, G. Boukettaya, "Study of a Low Voltage DC Micro Grid Based on a Solid-State Transformer Under Different Operating Conditions in Smart Grid Distribution", International Journal of Renewable Energy Research, Vol.14, No.4, December, 2024.
- [13] D. Amoozegar, "DSTATCOM modelling for voltage stability with fuzzy logic PI current controller," International Journal of Electrical Power & Energy Systems., vol.76, pp.129-135, 2016.
- [14] F. M. Dias, B. Canizes, H. Khodr, M. Cordeiro, "Distribution networks planning using decomposition optimization technique", Generation, Transmission & Distribution, IET, vol.9, no.12, pp.1409-1420, 2015.
- [15] S. Joseph, S. Ganguly "Allocation of DSTATCOM and DG in Distribution Systems to Reduce Power Loss using ESM Algorithm", 1st IEEE International Conference on Power Electronics, Intelligent Control and Energy Systems (ICPEICES-2016).
- [16] A. Belkaid, I. Colak, K. Kayışlı, R. Bayındır, "Improving PV system performance using high efficiency fuzzy logic control", 2020 8th International Conference on Smart Grid (icSmartGrid), 2020, pp. 152-156.
- [17] K. Sylevaster, C. Erdal, "Photovoltaic System Efficiency Enhancement with Thermal Management: Phase Changing Materials (PCM) with High Conductivity Inserts", International Journal of Smart Grid – ijSmartGrid, Vol 5, No 4 (2021).
- [18] M. Khalid, "Voltage Recovery Through Active-Reactive Coordination of Solar PV Inverters During Grid Fault", 11th IEEE International Conference on Renewable Energy Research and Applications, September 18-21, 2022, Istanbul, Turkey.
- [19] S. K. Injeti, "Butterfly optimizer-assisted optimal integration of REDG units in hybrid AC/DC distribution micro-grids based on minimum operational area", Journal of Electrical Systems and Information Technology, 8(13), pp-1-22, 2021.
- [20] M. Dixit, P. Kundu, H. R. Jariwala, "Incorporation of distributed generation and shunt capacitor in radial

- distribution system for techno-economic benefits”, *Engineering Science and Technology, an International Journal*, 20 (2017).
- [21] K. Miyamoto, S. Hamasaki, T. Daido, “Grid voltage control of energy storage system using dual active bridge converter”, 13th IEEE International Conference on Renewable Energy Research and Applications, November 9-13, Nagasaki, Japan.
- [22] Fahad Iqbal, Mohd Tauseef Khan, Anwar Shahzad Siddiqui, “Optimal placement of DG and DSTATCOM for loss reduction and voltage profile improvement”, *Alexandria Engineering Journal*, 2017.
- [23] A. Khodabakhshian, M.H. Andishgar, “Simultaneous placement and sizing of DGs and shunt capacitors in distribution systems by using IMDE algorithm”, *Int. J. Electr. Power Energy Syst.* 82 (2016) 599–607.
- [24] E. M. Ahmed, S. Rakocevic, M. Calasan, “BONMIN solver-based coordination of distributed FACTS compensators and distributed generation units in modern distribution networks”, *Ain Shams Engineering Journal* 13 (2022) 101664.
- [25] B. Ravindhar, B. S.Kumar, B Mangu, “Optimal coordinated voltage control in distribution systems with smart inverter-interfaced solar PV penetration: A discrete jellyfish search algorithm approach”, *International Journal of Renewable Energy Research*, Vol.14, No.1, March, 2024.